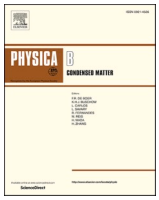
Physica B 714 (2025) 417420



Contents lists available at ScienceDirect

Physica B: Condensed Matter

journal homepage: www.elsevier.com/locate/physb





# Variation of the general mixing rule to explore the interphase in the AC electrical conductivity of polypropylene melt-mixed with as-grown carbon nanofiber composites

Najoia Aribou [a,*], Antonio J. Paleo [b,**], Jaime Oliveira da Silva [c], Carlos J. Tavares [d], M. Essaid Achour [a]

[a] Faculty of Sciences, Laboratory of Material Physics and Subatomic, Ibn Tofail University, Kenitra, Morocco
[b] 2C2T-Centre for Textile Science and Technology, University of Minho, Campus de Azurém, 4800-058, Guimaraes, Portugal
[c] CFisUC, Department of Physics, University of Coimbra, Rua Larga, 3004-516, Coimbra, Portugal
[d] Centre of Physics of Minho and Porto Universities (CF-UM-PT), University of Minho, 4804-533, Guimaraes, Portugal

ARTICLE INFO

*Keywords:*
Polypropylene
Carbon nanofibers
Interphase
AC electrical properties
Mixing rule model

ABSTRACT

A variation of the phenomenological mixing rule model is used to study the AC electrical conductivity of melt-extruded polypropylene (PP) compounds with varying carbon nanofibre (CNF) contents (0–1.4 vol %). The results show an insulator-conductor transition at 0.9 vol % CNF content, where the conductivity reaches ~$4 \times 10^{-8}$ S m$^{-1}$ at 430 Hz, while at the highest CNF loading of 1.4 vol % increases up to ~$6 \times 10^{-6}$ S m$^{-1}$, which makes them suitable as electrostatic dissipative (ESD) materials. From the modified mixing rule model, it is shown that the electrical conductivity ($\sigma_{int}$) and the volume constant ($k$), associated with the interphase, increase and decrease with the frequency, respectively, while the volume concentration of the interphase ($\phi_{int}$), despite increasing linearly with increasing vol. % of CNFs, decreases as frequencies increase, demonstrating that its effect becomes smaller as the frequency increases.

## 1. Introduction

Conductive polymer composites (CPCs) made with insulating polymers and filled with carbon materials are attracting growing interest in the development of high-performance multifunctional materials, particularly suited to applications in sectors such as energy, electronics, automotive, aeronautics, aerospace and packaging [1,2]. These materials combine lightness, flexibility and electrical conductivity, meeting a wide range of demanding requirements. The carbon materials most commonly used in CPCs include carbon nanotubes (CNTs), graphene, carbon nanofibres (CNFs), carbon fibers (CFs), and carbon black (CB) because they offer remarkable properties, particularly in terms of electrical conductivity, thermal stability and mechanical strength, making CPCs particularly effective in a variety of applications [3,4]. Among them, the significance in the market of packaging with antistatic electrical properties has prompted research towards the development of CPCs with conductivities from $10^{-11}$ to $10^{-4}$ S m$^{-1}$ in order to avoid the accumulation of charge and acquire electrostatic dissipative (ESD) protection [5]. Specifically, CNFs produced by chemical vapour deposition (CVD) are a compelling choice for CPCs thanks to their large surface area, their high strength and storage modulus and their excellent thermal and electrical properties [6,7]. In addition, polypropylene (PP) is widely used in engineering applications due to its moisture resistance, durability, cost-effectiveness, outstanding tensile properties and chemical resistance [8,9]. Thus, the combination of the two enables the development of CPCs suitable for advanced uses such as sensors and energy storage and harvesting devices in portable electronics [10,11]. However, predicting their electrical conductivity from the individual properties of their constituents remains a major challenge [12–14]. The percolation model shows that when the carbon material content exceeds a certain critical value $\phi_c$, CPCs show a jump of several orders of magnitude in their electrical conductivity [15], and it predicts two main regions; below and above that $\phi_c$. Below $\phi_c$, the electrical conductivity is reduced to the electrical conductivity of the insulating polymer matrix,

This article is part of a special issue entitled: Women in Condensed Matter and Materials 2024 published in Physica B: Condensed Matter.

* Corresponding author.
** Corresponding author.
*E-mail addresses:* najoiaaribou@yahoo.fr (N. Aribou), ajpaleovieito@2c2t.uminho.pt (A.J. Paleo).

https://doi.org/10.1016/j.physb.2025.417420
Received 25 March 2025; Received in revised form 13 May 2025; Accepted 23 May 2025
Available online 24 May 2025
0921-4526/© 2025 The Authors. Published by Elsevier B.V. This is an open access article under the CC BY license (http://creativecommons.org/licenses/by/4.0/).

since at low carbon material contents, the particles are not able to form a conductive network, while beyond $\phi_c$, the conductive network increases with increasing filler concentrations until the conductivity plateau is reached [16]. However, while experimental studies confirm that the percolation model generally works well in CPCs, it is also implicit in this model that no interphase between the conductive filler and the polymer matrix is considered [17]. In addition, other attempts result from the combination of effective medium (EMT) and percolation theories, as is the case with the generalized effective medium (GEM) model, have also been considered [18], where it is assumed that the CPC is a binary and homogeneous system, and there is a contact between the particles [19], and therefore this model also does not take into account the effect of the interphase. As conclusion, although all these attempts succeed in estimating the electrical conductivity of carbon-based CPCs reasonably well, a complete and accurate analysis of the effect of interphase in that last property is not yet achieved, when is generally assumed that polarization in the interphase is almost always present because the heterogeneity of this kind of systems [20], and therefore a description of the interphase characteristics is crucial for the understanding of CPCs simply because the fraction of the overall material which is in the vicinity of an interphase is high [21,22]. It is within this context that the motivation for this work arises, extending the discussion of previous work focusing on dielectric spectroscopy analysis of melt-extruded PP with as-grown CNFs compounds using universal power laws (UPL) [23], and the modified GEM model that includes the influence of the interphase between CNFs and PP [24]. In the latter work, not only was it possible to quantify the conductivity and volume fraction due to the interphase, but a decrease in that conductivity and volume fraction with increasing frequency was also detected. Herein, the room temperature AC electrical conductivity results already presented in those earlier studies are now estimated using a simple mixing rule as an alternative phenomenological approach. In addition, the variation of that mixing rule, which consider the influence of the interphase between the CNFs and the PP, is also examined here. As will be seen below, despite its simplicity, good agreement has been found with the experimental measurements, and noticeably, this new approach leads to the same conclusions as in the previous work, confirming the effect of the interphase on the electrical properties of these particular compounds.

## 2. Materials and methods

### 2.1. Materials

Polypropylene (Daplen™ Borealis EE002AE) and as-received PR 25 AG carbon nanofibers (ASI, Cedarville, OH, USA) were used to produce the compounds PP/CNF. The CNFs, produced by CVD, have dimensions of 30–100 μm in length, with diameters of 100–200 nm, which include hollow cores of 30–90 nm in diameter, and estimated electrical conductivities of $10^3$ S $m^{-1}$. More detailed information on them can be found in previous reports [25].

### 2.2. Polymer composites processing

The samples were manufactured by melt-extrusion with a twin-screw extruder consisting of two screws of diameters of 13 mm and barrel lengths of 31 cm. The screw configuration was designed to achieve high shear mixing and long residence times during processing [23], since with this choice good dispersions were achieved for Pyrograf® III PR 19 LHT XT and PR 24 LHT XT grades in PP [26]. In particular, rotation speed of 50 rpm and barrel temperatures of 190 °C were selected for the process. Further details on the melt extrusion conditions can be found elsewhere [27]. After the extrusion process, the PP/CNF composite films with volume concentrations from 0 to 1.4 vol % were pelletized and formed into specimens with suitable geometries for various analyses.

### 2.3. Characterization

Morphological analysis of PP/CNF composites were carried out in an Ultrahigh resolution Field Emission Gun Scanning Electron Microscopy (FEG-SEM), NOVA 200 Nano SEM, FEI Company at SEMAT/UM. The specimens were broken under cryogenic conditions and, before testing, they were coated by sputter deposition with a thin layer of gold.

For the AC electrical analysis, films of geometries of 0.5 × 10 × 10 $mm^3$ with Au contacts deposited on both sides by thermal evaporation were used. The capacitance $C(\omega)$ and dielectric losses tan $\delta(\omega)$ were acquired with a Quadtech1929 LCR (Maynard, WI, USA) at frequencies from 200 Hz to 2 MHz under an applied signal of 0.5 V. The real $\varepsilon'(\omega)$ and the imaginary $\varepsilon''(\omega)$ components of the complex dielectric permittivity $\varepsilon^*(\omega)$ were after calculated using:

$$\varepsilon(\omega) = \frac{C(\omega).d}{A.\varepsilon_0} \tag{1}$$

$$\varepsilon''(\omega) = \varepsilon(\omega).\tan\delta \tag{2}$$

here, $d$ is the thickness, $A$ is the surface area, $\varepsilon_0$ is the permittivity of vacuum, and $\omega$ is the circular frequency. The AC electrical conductivity $\sigma_{AC}(\omega)$ was obtained using:

$$\sigma_{AC}(\omega) = \omega\varepsilon_0\varepsilon''(\omega) \tag{3}$$

The DC electrical conductivity $\sigma_{DC}$ was measured by a picoammeter Keitheley model 6487 and a digital-control DC power supply TENMA model 72–10495. The power supply was set with an output of 1 V, and resistivities of each specimen was obtained through the arithmetic mean of 10 tests [23].

## 3. Results and discussion

### 3.1. Morphological analysis

SEM micrographs at lower and higher magnification of PP/CNF composites with 0.9 % vol. of CNFs (Fig. 1) show that the fillers are well dispersed and distributed throughout the PP without the presence of aggregates. It should be noted that the CNFs used in this study, labelled PR 25 AG, unlike the commercial grade Pyrograf® III CNFs, are not heat treated after production, resulting in less graphitised outer layers, nor are they subjected to any debulking method, which, according to the manufacturer, would probably contribute to their poorer dispersion in the polymer matrix as it was demonstrated in a previous works [24,27], where the appearance of agglomerates is evident from the lowest CNF loadings of 0.2 vol %, from which agglomerates increase as more and more CNFs are incorporated into the extrusion process until a point is reached where the formation of the paths necessary for electrical conduction is promoted.

### 3.2. AC/DC conductivity analysis

The AC/DC electrical conductivity of the PP/CNF films illustrated in Fig. 2 has already been analyzed in previous works [25]. In general, $\sigma_{AC}$ shows a clear increase with CNF concentration at all frequencies, attributed to the conduction through tunneling and hopping mechanisms [28]. The AC conductivity of unfilled PP and PP composites with up to 0.9 vol % of CNFs shows a linear trend with frequency, which is a good demonstrator of their quasi-insulative characteristics. On the contrary, the $\sigma_{AC}$ becomes independent at low frequencies up to the critical frequency $f_c$ (~43 kHz) for PP composites with a CNF loading of 1.4 vol %. It is noticed that this frequency-independent regime becomes visible between 0.9 and 1.4 vol%, demonstrating a change from the non-conducting to the conducting behavior due to the creation of a network of contacts of CNFs within the PP [29]. The DC electrical conductivity $\sigma_{DC}$ of the PP/CNF composites is presented in Fig. 2(b), and

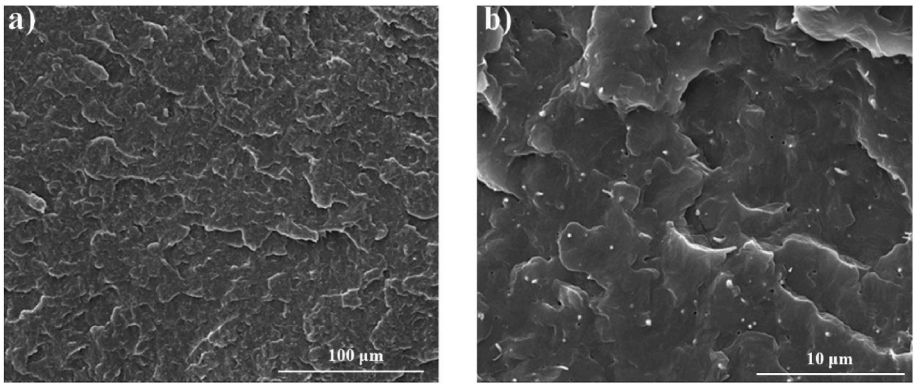



**Fig. 1.** SEM micrographs of PP filled with 0.9 vol % of CNFs.

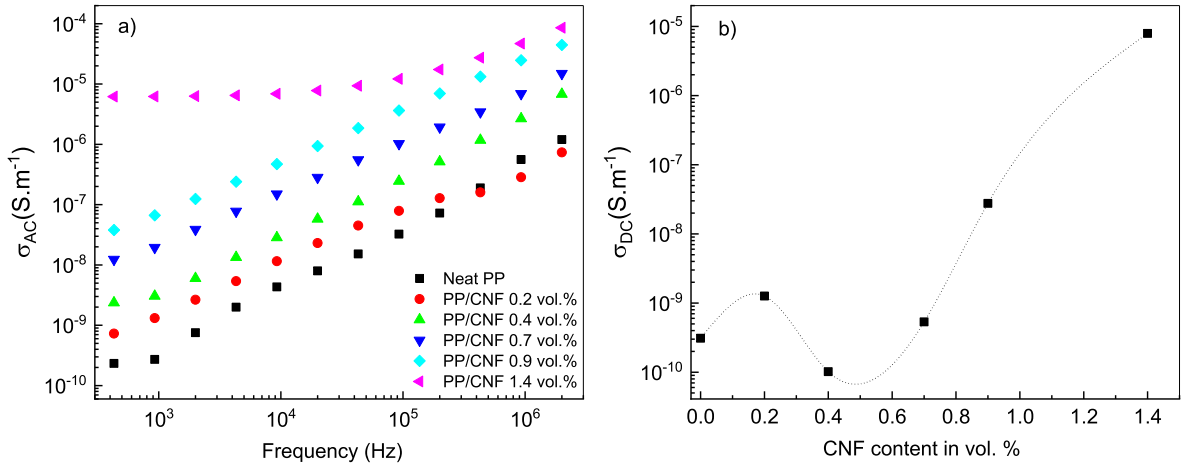



**Fig. 2.** AC/DC electrical conductivity of PP/CNF composites: (a) $\sigma_{AC}$ as a function of vol. % of CNFs and frequency; (b) $\sigma_{DC}$ as function of vol. % of CNFs [23,24]. (Dotted line serves for guiding the eyes).

it shows that for CNF contents ranging from 0.2 to 0.7 vol% there are no significant variations with respect to unfilled PP (~$10^{-10}$ S m$^{-1}$), indicating that CNFs do not significantly influence $\sigma_{DC}$ at these concentrations. However, for PP composites with 1.4 vol% of CNFs, $\sigma_{DC}$ increases in four orders of magnitude (~$8 \times 10^{-6}$ S m$^{-1}$). Thus, $\sigma_{DC}$ confirms the transition from insulating to conductive behaviour between PP/CNF composites with 0.9 and 1.4 vol% CNF previously observed for $\sigma_{AC}$. It is noticed that this largest value of $\sigma_{DC}$ is considerably smaller than the one reported for PP/CNF composites made from Pyrograf® III PR 24 LHT XT CNFs, which showed a $\sigma_{DC}$ value of ~ 16 S m$^{-1}$ for the same CNFs concentration (Table 1) [30]. This worse result can be explained by the absence of the thermal post-treatment for this type of CNFs (PR 25 AG), which would contribute to the ordering of their outermost layers, thus facilitating the increase of the electrical conductivity [31]. In addition, the lack of a debulking method to decrease the bulk density of CNFs, as well as their lower aspect ratios with respect to commercial Pyrograf® III grades, may explain the smaller $\sigma_{DC}$ values observed for these PP/CNF composites. However, it is also possible to find worse conductivities in the literature for melt-extruded PP-based composites with similar contents of Pyrograf® III carbon nanofibers, as can be seen in the comparative Table 1 for Pyrograf® III grades PR 25 PS XT and PR 24 HHT XT.

**Table 1**
$\sigma_{DC}$ values of PP/CNF composites based on Pyrograf® III CNFs. The term * means that authors do not specify the exact grade.

| CNF type | Method | Content | $\sigma_{DC}$ (S m$^{-1}$) | Ref. |
|---|---|---|---|---|
| Pyrograf® III (PR 25 PS XT) | Melt mixing | 5 wt % | $1 \times 10^{-10}$ | [32] |
| Pyrograf® III (PR 19 LHT XT) | Melt extrusion | 3 wt % | 1 | [33] |
| Pyrograf® III (PR 24 LHT XT) | Melt extrusion | 3 wt % | 16 | [30] |
| Pyrograf® III* | Melt extrusion | 3 wt % | $1 \times 10^{-6}$ | [34] |
| Pyrograf® III (PR 24 HHT XT) | Melt mixing | 4 wt % | $7 \times 10^{-8}$ | [35] |
| PR 25 AG | Melt extrusion | 1.4 vol % (3 wt %) | $8 \times 10^{-6}$ | This work |

It should be noticed that $\sigma_{DC}$ can be fitted by the percolation theory with the power law relation $(\phi - \phi_c)^t$, which connects $\sigma_{DC}$ to the critical volume fraction $\phi_c$, an $t$ is a critical exponent linked to the dimensionality of the CNF network [36]. However, under the processing conditions presented in this work, it has not been possible to produce PP/CNF composites with CNF contents higher than 1.4 vol %, which may be evidence that the heat treatment that commercial Pyrograf® III grades receive is positive to better disperse them in polypropylene with this methodology.

### 3.3. AC/DC conductivity analysis by a general mixing rule

As demonstrated in previous work, the mixing rule is an alternative phenomenological approach to estimation of electrical conductivity in conductor-insulator composites, which can be written as follows [37]:

$$\sigma^n = (1-\phi)\sigma_m^n + \phi\sigma_f^n \quad (4)$$

where for this study, the parameters $\sigma$, $\sigma_m$ and $\sigma_f$ represent the electrical conductivity of PP/CNF composites, PP, and CNFs respectively, $\phi$ denotes the volume concentration of CNFs, and the exponent $n$ can be determined by fitting Eq. (4) to the experimental values of $\sigma_{AC}$. It is also noted that the model predicts $n$ values between −1 and 1, where $n = -1$ corresponds to the case where the CNFs are oriented perpendicular to the direction of the electrical current (lower-bound of $\sigma$), while $n = 1$ corresponds to the case of the CNFs are oriented in parallel to the electrical current direction (upper-bound of $\sigma$) [38]. From the experimental results, a $\sigma_m$ value of $10^{-10}$ S m$^{-1}$ has been used in Eq. (4) for PP, while for CNFs, $\sigma_f$ value of $10^3$ S m$^{-1}$ has been considered [39]. Accordingly, Fig. 3(a) shows the $\sigma_{AC}$ of PP/CNF composites at 93 kHz plotted with Eq. (4) as function of the CNF vol. %. In particular, the dashed blue line labelled as $n$ universal in Fig. 3(a) corresponds to the fitting when 1/3 is used as representative arithmetic mean between the two limiting bounds [37], while the dashed red line corresponds to the fitting when $n$ is adjusted exactly to −1.1. Similarly, the exponents $n$ for the remaining frequencies have been adjusted and the results are shown in Fig. 3(b), where, interestingly, as frequency increases, $n$ approaches the lower bound −1 assumed by the model.

### 3.4. AC/DC conductivity analysis by including interphase in the general mixing rule

The latter results, i.e., the deviation of the exponent $n$ from the universal values, leads to hypothesize whether the interphase between the CNFs and the PP, as depicted in Fig. 4, can play a role in the $\sigma_{AC}$ of PP/CNF composites. To address this hypothesis, Eq. (4) is modified in this study by incorporating the electrical conductivity $\sigma_{int}$ and volume fraction $\phi_{int}$ corresponding to the interphase as follows:

$$\sigma^n = (1 - \phi - \phi_{int})\sigma_m^n + \phi_{int}\sigma_{\text{int}}^n + \phi\sigma_f^n \quad (5)$$

where $\sigma_{int}$, represents the effective conductivity of this interphase, which is generally lower than that of the pure filler but higher than that of the matrix, and $\phi_{int}$ represents the effective volume fraction of the interphase, which can impact the development of conductive networks. It is noticed that $\phi_{int}$ depends on the filler concentration $\phi$ as well as on the critical parameter $k$ given by Todd and Vo as [40,41]:

$$\phi_{\text{int}} = (k\phi)\left(\frac{1-\phi}{1+k\phi}\right) \quad (6)$$

It should be noticed that a small $k$ indicates negligible interaction between the polymer and the CNFs, while a large $k$ indicates just the

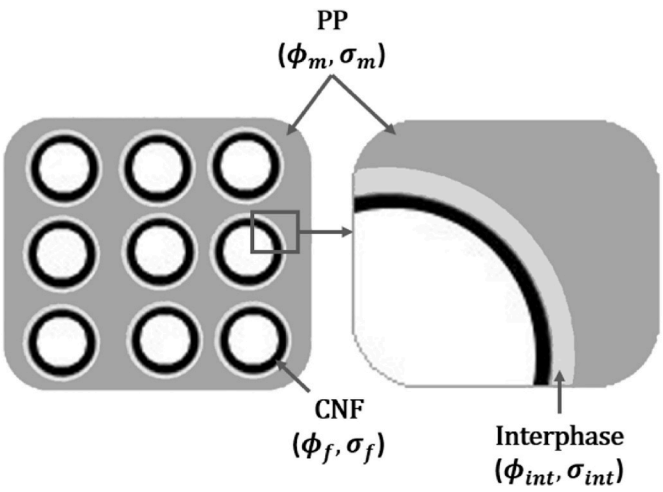



**Fig. 4.** Schematic representation of interphase in PP/CNF composites.

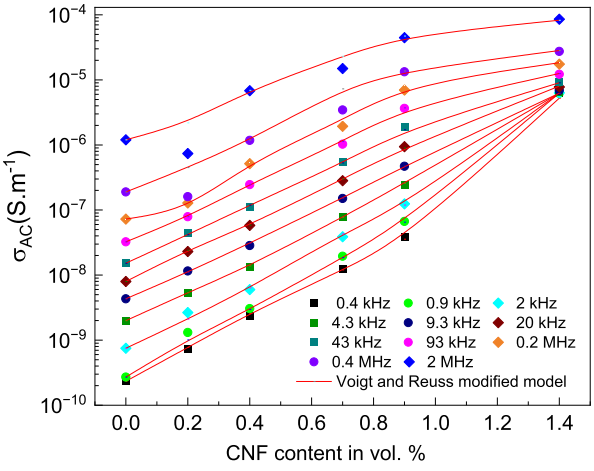



**Fig. 5.** Experimental (full symbols) and fittings (red lines) of $\sigma_{AC}$ by the modified model (Eq. (5)) for PP/CNF composites. (For interpretation of the references to colour in this figure legend, the reader is referred to the Web version of this article.)

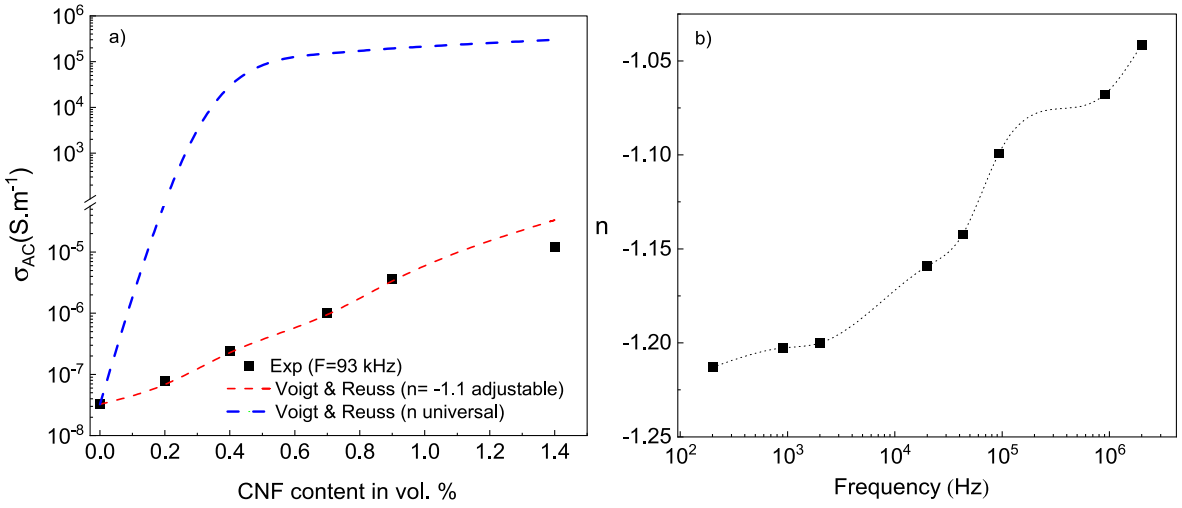



**Fig. 3.** $\sigma_{AC}$ of PP/CNF composites: (a) experimental (full symbols) and fittings with Eq. (4) (dashed lines) of $\sigma_{AC}$ at 93 kHz; (b) Fitted exponents $n$ determined by Eq. (4) at different frequencies. (Dotted line serves for guiding the eyes).

opposite [42]. Consequently, $\sigma_{AC}$ results shown in Fig. 5 are obtained resolving numerically Eq. (5) through an interactive process, where $k$ and $\sigma_{int}$ are adjustable parameters, and $n \sim 1/3$ is used. In particular for PP composites with 1.4 vol % of CNFs, values of $\sigma_{int}$, $k$, and $\phi_{int}$ of $6.17 \pm 0.01 \times 10^{-9}$ S m$^{-1}$, $0.56 \pm 0.01$, and 0.8 vol % are calculated at 0.4 kHz, and values of $\sigma_{int}$, $k$, and $\phi_{int}$ of $9.94 \pm 0.03 \times 10^{-7}$ S m$^{-1}$, $0.15 \pm 0.02$, and 0.2 vol % are calculated at 93 kHz, respectively.

Similarly, the values of $\sigma_{int}$ and $k$ for PP/CNF composites are calculated and presented in Fig. 6(a) and (b), respectively, for the rest of frequencies. Fig. 6(a) shows an increase of $\sigma_{int}$ with increasing frequency, which agrees with the increase of $\sigma_{AC}$ with frequency observed in Fig. 2(a). However, as shown in Fig. 6(b), the critical parameter $k$ decreases with increasing frequency, suggesting that the interaction between PP chains and CNFs is weaker at higher frequencies. Notably, this finding matches well with previous work on polymers reinforced with carbon black particles, where the same inverse relationship between $k$ and frequency is observed [43]. In that work, the authors attributed this to the increasing energy of the electrons, which results in a higher probability of hopping between nearest neighbours CBs. In turn, Fig. 6(c) shows the variation of $\phi_{int}$ as a function of vol. % CNF concentration, calculated according to Eq. (5) for various frequencies, where it can be seen that $\phi_{int}$ increases linearly with increasing CNF concentration for all frequencies, which seems logical, since as the concentration of CNFs increases, it is to be expected that the interphase zone will also increase, and it decreases as frequencies increase. Previous work has observed the same phenomenon (the linear increase of mass fraction corresponding to interphase with increasing CNF concentration), and in addition it suggests that the thickness of the interphase is not significantly affected by the concentration of CNFs [44]. In that study, on the basis of these facts, and from considering the densities of CNFs and the polypropylene, and the diameter and length of the CNFs, they demonstrated the existence of a two-layer interface in melt-blended PP/CNF composites made from a similar type of CNF (PR 24 AG), where the outer and inner layers of the interphase are estimated to be $10^2$ nm and $10^0$ nm thick, respectively. Based on the same hypothesis, and considering that CNFs in this study have slightly larger diameters with the same length, we can consider that we should have a thickness in the same order of $10^2$ nm for our composites. It is worth recalling that similar behaviour of $\sigma_{int}$, $k$ and $\phi_{int}$ as a function of frequency using a modification of the generalized effective medium (GEM) model, which also included the interphase, has already been discussed [24]. In particular, Table 2 includes $\sigma_{int}$ calculated with Eq. (5) and GEM model from previous work. Therefore, from the results of the former [24] and the present study, it can be deduced that this decrease of $k$ and $\phi_{int}$ with increasing frequency should be related to a lesser effect of the interphase on the AC conductivity, which facilitates the electron hopping between

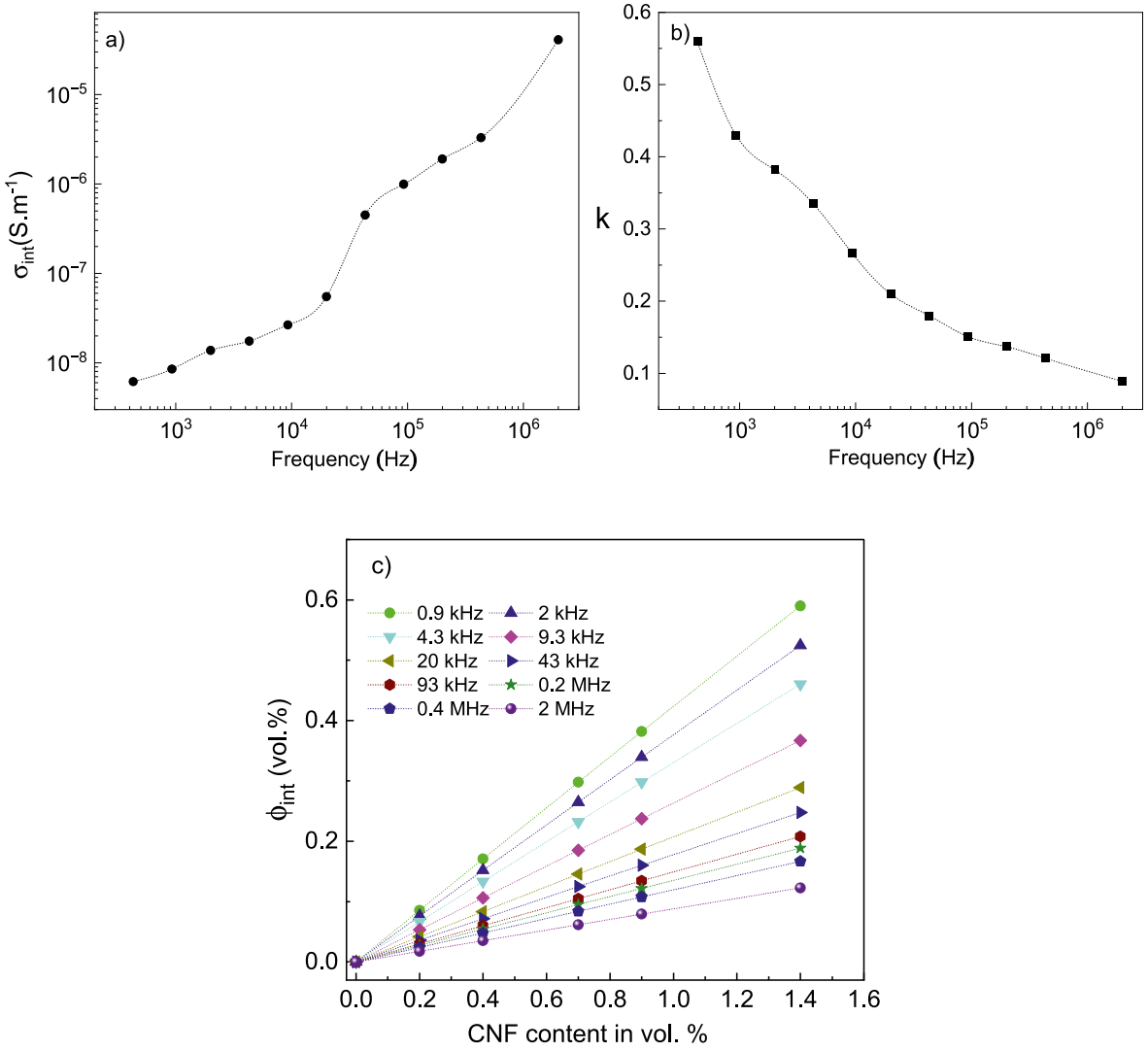



**Fig. 6.** Parameters obtained by the modified model (Eq. (5)): (a) $\sigma_{int}$, (b) $k$, and (c) $\phi_{int}$ of all PP/CNF composites as function of frequency. (Dotted lines serve for guiding the eyes).

**Table 2**
$\sigma_{int}$ values estimated by GEM model [24] and Eq. (5) in this work of PP/CNF composites.

| F (kHz) | $\sigma_{int}$ by GEM (S m$^{-1}$) [24] | $\sigma_{int}$ by Eq. (5) (S m$^{-1}$) |
|---|---|---|
| 9.3 | $1.1 \times 10^{-8}$ | $2.6 \times 10^{-8}$ |
| 20 | $7.6 \times 10^{-8}$ | $5.5 \times 10^{-8}$ |
| 43 | $9.5 \times 10^{-8}$ | $4.5 \times 10^{-7}$ |
| 93 | $1.3 \times 10^{-7}$ | $9.9 \times 10^{-7}$ |
| 200 | $6.0 \times 10^{-7}$ | $1.9 \times 10^{-6}$ |
| 400 | $8.1 \times 10^{-6}$ | $3.3 \times 10^{-6}$ |
| 2000 | $2.9 \times 10^{-5}$ | $4.1 \times 10^{-5}$ |

the CNFs, and, consequently, it should explain that the values of $\sigma_{AC}$ and $\sigma_{int}$ become closer together as the frequency is increasing.

## 4. Conclusions

The AC electrical conductivity as function of frequency ($\sigma_{AC}$) of melt-extruded polypropylene (PP) composites with carbon nanofibers (CNFs) from 0 to 1.4 vol % is investigated. The results show an insulating–conducting change near 0.9 vol % of CNFs, where the PP/CNF composites with highest load (1.4 vol %) shows the largest electrical conductivity. The $\sigma_{AC}$ is analyzed using the simple mixing rule model as well as a modified model that considers the interphase effect between CNFs and PP. While the unmodified model shows limited applicability across all vol. % of CNFs, the modified model accurately fits the $\sigma_{AC}$ values, allowing for the specific estimation of parameters corresponding to the interphase such as the electrical conductivity ($\sigma_{int}$), and the volume concentration ($\phi_{int}$). From the analysis it is concluded that the interphase between the PP and the CNFs substantially decreases its effect on the $\sigma_{AC}$ of their PP/CNF composites with the increase in frequency.

## CRediT authorship contribution statement

**Najoia Aribou:** Writing – original draft, Visualization, Validation, Methodology, Investigation, Formal analysis, Conceptualization. **Antonio J. Paleo:** Writing – review & editing, Validation, Supervision, Resources, Project administration, Methodology, Investigation, Funding acquisition, Formal analysis, Data curation, Conceptualization. **Jaime Oliveira da Silva:** Writing – review & editing, Visualization, Supervision, Investigation, Formal analysis. **Carlos J. Tavares:** Writing – review & editing, Resources, Methodology, Investigation, Formal analysis, Data curation. **M. Essaid Achour:** Validation, Supervision, Methodology, Investigation, Formal analysis, Conceptualization.

## Declaration of competing interest

The authors declare that they have no known competing financial interests or personal relationships that could have appeared to influence the work reported in this paper.

## Acknowledgments

A. J. Paleo would like to acknowledge the European Regional Development Fund through the Operational Competitiveness Program and the National Foundation for Science and Technology of Portugal (FCT) under the projects UID/CTM/00264/2020 of Centre for Textile Science and Technology (2C2T) on its components base and programmatic. C.J. Tavares acknowledges the funding from FCT/PIDDAC through the Strategic Funds project reference UIDB/04650/2020–2024.

## Data availability

Data will be made available on request.

## References

[1] T. Hassan, A. Salam, A. Khan, S.U. Khan, H. Khanzada, M. Wasim, M.Q. Khan, I. S. Kim, Functional nanocomposites and their potential applications: a review, J. Polym. Res. 28 (2021) 36.
[2] M. Rahaman, A. Aldalbahi, L. Nayak, R. Giri, Electrical conductivity of polymer–carbon composites: effects of different factors, in: M. Rahaman, D. Khastgir, A.K. Aldalbahi (Eds.), Carbon-Containing Polymer Composites, Springer Singapore, Singapore, 2019, pp. 159–210.
[3] R.M. Mutiso, K.I. Winey, Electrical properties of polymer nanocomposites containing rod-like nanofillers, Prog. Polym. Sci. 40 (2015) 63–84.
[4] C. Min, X. Shen, Z. Shi, L. Chen, Z. Xu, The electrical properties and conducting mechanisms of carbon nanotube/polymer nanocomposites: a review, Polym.-Plast. Technol. Eng. 49 (2010) 1172–1181.
[5] Q. Wang, T. Wang, J. Wang, W. Guo, Z. Qian, T. Wei, Preparation of antistatic high-density polyethylene composites based on synergistic effect of graphene nanoplatelets and multi-walled carbon nanotubes, Polym. Adv. Technol. 29 (2018) 407–416.
[6] J.-P. Tessonnier, D. Rosenthal, T.W. Hansen, C. Hess, M.E. Schuster, R. Blume, F. Girgsdies, N. Pfänder, O. Timpe, D.S. Su, R. Schlögl, Analysis of the structure and chemical properties of some commercial carbon nanostructures, Carbon 47 (2009) 1779–1798.
[7] F. Ghaemi, M. Ali, R. Yunus, R.N. Othman, Chapter 1 - synthesis of carbon nanomaterials using catalytic chemical vapor deposition technique, in: S.A. Rashid, R.N.I. Raja Othman, M.Z. Hussein (Eds.), Synthesis, Technology and Applications of Carbon Nanomaterials, Elsevier, 2019, pp. 1–27.
[8] H. Shaikh, S.K.H. Gulrez, A. Anis, A.M. Poulose, P.E.H. Qua, M.K. Yadav, S.M. Al-Zahrani, Progress in carbon fiber and its polypropylene- and polyethylene-based composites, Polym.-Plast. Technol. Eng. 53 (2014) 1845–1860.
[9] S. Han, S. Chen, F. Jiao, Insulating polymers for flexible thermoelectric composites: a multi-perspective review, Compos. Commun. 28 (2021) 100914.
[10] H. Tao, M. Yan, L. Zhang, Z. Zou, B. Han, H. Dong, B. Zhu, X. Li, Progress in preparation, processing, and application of high dielectric polypropylene matrix composite materials, Polym. Compos. 45 (2024) 4819–4838.
[11] Jamiru Adeoti, Suleiman Adegbola, Aramide Abdullahi, Selection criteria of polymer nanocomposites for electrical energy storage applications: a concise review, Express Polym. Lett. 19 (2025) 208–229.
[12] S.A. Elhad Kassim, M.E. Achour, L.C. Costa, F. Lahjomri, Prediction of the DC electrical conductivity of carbon black filled polymer composites, Polym. Bull. 72 (2015) 2561–2571.
[13] F. Lux, Models proposed to explain the electrical conductivity of mixtures made of conductive and insulating materials, J. Mater. Sci. 28 (1993) 285–301.
[14] S.H. Foulger, Electrical properties of composites in the vicinity of the percolation threshold, J. Appl. Polym. Sci. 72 (1999) 1573–1582.
[15] B. Nigro, C. Grimaldi, P. Ryser, Tunneling and percolation transport regimes in segregated composites, Phys. Rev. E 85 (2012) 011137.
[16] R. Taherian, M.J. Hadianfard, A.N. Golikand, A new equation for predicting electrical conductivity of carbon-filled polymer composites used for bipolar plates of fuel cells, J. Appl. Polym. Sci. 128 (2013) 1497–1509.
[17] G.V. Aldica, M.L. Ciurea, D.M. Chipara, A.M. Lepadatu, K. Lozano, I. Stavarache, S. Popa, M. Chipara, Isotactic polypropylene–vapor grown carbon nanofibers composites: electrical properties, J. Appl. Polym. Sci. 134 (2017) 45297.
[18] D.S. McLachlan, M. Blaszkiewicz, R.E. Newnham, Electrical resistivity of composites, J. Am. Ceram. Soc. 73 (1990) 2187–2203.
[19] I. Bouknaitir, N. Aribou, S.A. Elhad Kassim, M. El Hasnaoui, B.M.G. Melo, M. E. Achour, L.C. Costa, Electrical properties of conducting polymer composites: experimental and modeling approaches, Spectrosc. Lett. 50 (2017) 196–199.
[20] G.M. Tsangaris, G.C. Psarras, N. Kouloumbi, Electric modulus and interfacial polarization in composite polymeric systems, J. Mater. Sci. 33 (1998) 2027–2037.
[21] E.J. Bailey, K.I. Winey, Dynamics of polymer segments, polymer chains, and nanoparticles in polymer nanocomposite melts: a review, Prog. Polym. Sci. 105 (2020) 101242.
[22] C. Brosseau, Modeling the interface between phases in dense polymer-carbon black nanoparticle composites by dielectric spectroscopy: where are we now and what are the opportunities? Macromol. Theory Simul. 33 (2024) 2400009.
[23] A.J. Paleo, Z. Samir, N. Aribou, Y. Nioua, M.S. Martins, M.F. Cerqueira, J. Agostinho Moreira, M.E. Achour, Dielectric spectroscopy of melt-extruded polypropylene and as-grown carbon nanofiber composites, Eur. Phys. J. E 44 (2021) 73.
[24] A.J. Paleo, N. Aribou, Y. Nioua, Z. Samir, L. Fernandes, J.Agostinho Moreira, M. E. Achour, Electrical properties of melt-mixed polypropylene and as-grown carbon nanofiber composites: analysis of their interphase via the AC conductivity modeling, J. Compos. Mater. 56 (2022) 1879–1889.
[25] A.J. Paleo, Z. Samir, N. Aribou, Y. Nioua, J.Agostinho Moreira, M.E. Achour, Electrical properties of polypropylene-based composites melt-processed with as-grown carbon nanofibers, in: F. Dogan (Ed.), Conductivity and Thermoplastic Elastomer Properties of Polypropylene Materials, IntechOpen, Rijeka, 2022.
[26] A.J. Paleo, X. García, L. Arboleda-Clemente, F.W. Van Hattum, M.J. Abad, A. Ares, Enhanced thermal conductivity of rheologically percolated carbon nanofiber reinforced polypropylene composites, Polym. Adv. Technol. 26 (2015) 369–375.
[27] A.J. Paleo, V. Sencadas, F.W.J. van Hattum, S. Lanceros-Méndez, A. Ares, Carbon nanofiber type and content dependence of the physical properties of carbon nanofiber reinforced polypropylene composites, Polym. Eng. Sci. 54 (2014) 117–128.

[28] M.H. Al-Saleh, Influence of carbon nanotubes purity on the properties of carbon nanotubes/low-density polyethylene composites, J. Macromol. Sci. B 61 (2022) 611–621.
[29] M. Taj, S.R. Manohara, Significantly enhanced electrical and dielectric properties, and thermal stability of poly(3,4-ethylenedioxythiophene) coated on functionalized multiwalled carbon nanotubes, Synth. Met. 269 (2020) 116572.
[30] A.J. Paleo, B. Krause, M.F. Cerqueira, M. Melle-Franco, P. Pötschke, A.M. Rocha, Thermoelectric properties of polypropylene carbon nanofiber melt-mixed composites: exploring the role of polymer on their Seebeck coefficient, Polym. J. 53 (2021) 1145–1152.
[31] K.L. Stokes, T.M. Tritt, W.W. Fuller-Mora, A.C. Ehrlich, R.L. Jacobsen, Electronic transport properties of highly conducting vapor-grown carbon fiber composites, in: Fifteenth International Conference on Thermoelectrics. Proceedings ICT '96, 1996, pp. 164–167.
[32] Z. Samir, A.J. Paleo, N. Aribou, Y. Nioua, J.O. da Silva, M.F. Cerqueira, J. A. Moreira, M.E. Achour, Dielectric spectroscopy of melt-mixed polypropylene and pyrolytically stripped carbon nanofiber composites, J. Compos. Sci. 6 (2022) 368.
[33] A.J. Paleo, F.W.J. van Hattum, J. Pereira, J.G. Rocha, J. Silva, V. Sencadas, S. Lanceros-Méndez, The piezoresistive effect in polypropylene—carbon nanofibre composites obtained by shear extrusion, Smart Mater. Struct. 19 (2010) 065013.
[34] G. Sui, S. Jana, W.H. Zhong, M.A. Fuqua, C.A. Ulven, Dielectric properties and conductivity of carbon nanofiber/semi-crystalline polymer composites, Acta Mater. 56 (2008) 2381–2388.
[35] J.M. Muñoz-Ávila, S. Sánchez-Valdes, I. Yáñez-Flores, O.S. Rodriguez-Fernandez, M.G. Neira-Velázquez, E. Hernández-Hernández, S. Flores-Gallardo, F. Avalos-Belmontes, T. Lozano-Ramírez, A. Morales-Cepeda, P.G. Lafleur, Influence of carbon nanofiber functionalization and compatibilizer on the physical properties of carbon nanofiber reinforced polypropylene nanocomposites, Polym. Compos. 39 (2018) 3575–3585.
[36] D. Stauffer, A. Aharony, Introduction to Percolation Theory, second ed., 2018.
[37] N.F. Uvarov, Estimation of composites conductivity using a general mixing rule, Solid State Ionics 136–137 (2000) 1267–1272.
[38] A. Wiśniewska, S. Hernik, A. Liber-Kneć, H. Egner, Effective properties of composite material based on total strain energy equivalence, Compos. B Eng. 166 (2019) 213–220.
[39] M.H. Al-Saleh, U. Sundararaj, A review of vapor grown carbon nanofiber/polymer conductive composites, Carbon 47 (2009) 2–22.
[40] H.T. Vo, M. Todd, F.G. Shi, A.A. Shapiro, M. Edwards, Towards model-based engineering of underfill materials: CTE modeling, Microelectron. J. 32 (2001) 331–338.
[41] M.G. Todd, F.G. Shi, Characterizing the interphase dielectric constant of polymer composite materials: effect of chemical coupling agents, J. Appl. Phys. 94 (2003) 4551–4557.
[42] X. Liu, Y. Wu, X. Wang, R. Li, Z. Zhang, Effect of interphase on effective permittivity of composites, J. Phys. Appl. Phys. 44 (2011) 115402.
[43] N. Aribou, Y. Nioua, I. Bouknaitir, M. El Hasnaoui, M.E. Achour, L.C. Costa, Prediction of filler/matrix interphase effects on AC and DC electrical properties of carbon reinforced polymer composites, Polym. Compos. 40 (2019) 346–352.
[44] M. Chipara, K. Lozano, A. Hernandez, M. Chipara, TGA analysis of polypropylene–carbon nanofibers composites, Polym. Degrad. Stabil. 93 (2008) 871–876.